2000

The Effects of Pressure on Fracture of a Rubbery Particulate Composite

T. C. Miller and **C. T. Liu**
Air Force Research Laboratory, AFRL/PRSM, 10 E. Saturn Blvd., Edwards AFB, CA

Introduction

Rubbery particulate composites used in aerospace consist of a rubbery matrix with a large volume of embedded particles. Cracks may form in these composites and cause catastrophic failure of the component. If we can better predict their fracture, expensive components with questionable cracks may be usable. Research on fracture of these composites has been ongoing but has been inhibited by their unique behavior. The large deformations and the material inhomogeneity make using conventional experimental techniques and related analytical methods difficult, and matrix viscoelasticity requires careful consideration of strain rates and temperatures. Most experimental research on the fracture of rubbery particulate composites has been under ambient pressure conditions [1-4], although the effect of pressure is important since service conditions involve high pressure during critical portions of the component life. This work studies the pressure effect on a particulate composite. We tested the composite for fracture properties in a pressure chamber, and investigated the initiation of crack growth and the growth rate.

Experimental Setup

The material used for the experiments was a particulate composite containing a large volume fraction (60-80%) of hard particles embedded in a rubbery matrix. Due to the nature of the matrix material, the strain rates and test temperatures for the tensile and fracture tests had to be similar (0.0667 mm/mm/min and 25 °C, respectively). We tested both single edge notched tension (SENT) and surface cracked specimens. For the SENT specimens, we tested various thicknesses and crack sizes (see Fig. 1 and Table 1). The surface cracked specimens were all identical (see Fig. 1) and were tested for comparison with the SENT specimen results. Testing took place inside a pressure chamber using nitrogen gas to apply a pressure of 6894 kPa. The pressure chamber has sight ports for observing the crack behavior during the test. We positioned a light at one port and a video camera at the other, so that we could observe and record the crack behavior during the test. A digital time encoder imprinted times onto the videotape. We noted the time at which the test started and used this to synchronize the videotape images with the testing machine data to obtain the specimen displacement, load, and crack size at many times for each test.

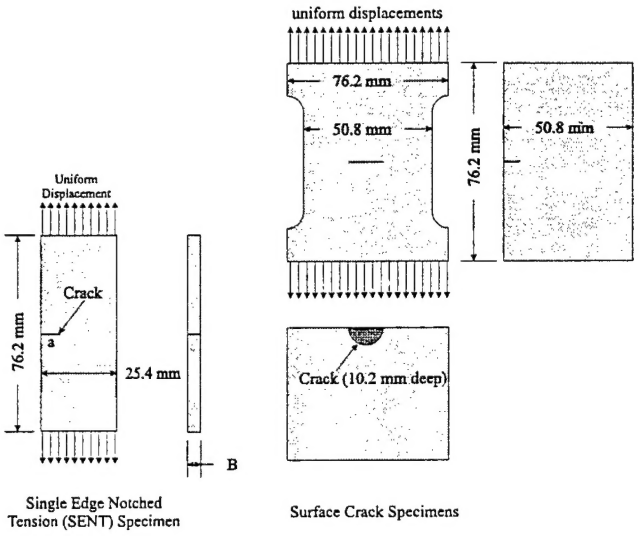

Figure 1 — Specimens Used in Pressurized Fracture Tests

Table 1 — Test matrix used for pressurized fracture tests

	a_0 [mm] / B [mm]	2.54	7.62	12.70
Number of SENT specimens tested	**5.08**	3	3	3
	12.70	3	3	3
	38.10	3	3	3
Number of surface crack specimens	6			

To obtain data for the crack growth initiation, we examined the videotape to find when growth began and took the loads and displacement from the synchronized data. This initiation event is detected by closely monitoring the crack tip using the video camera. At growth initiation, the advance of the crack tip can easily be seen, and is clearly distinguishable from any previous blunting behavior. Next we monitored the crack size and correlated it with loads and displacements. We measured the crack on the videotape images from the time of growth

initiation until the maximum load in regular intervals of either one or two seconds.

Results and Discussion

Finite Element Analysis

We used finite element results to find the stress intensities for each data point. The elements used the hydrostatic component of stress as a variable in addition to the displacement components at each of the nodes. This type of element (*a hybrid element*) is necessary due to the incompressibility of the composite materials [5]. Our analysis used uniform displacement boundary conditions (to match the test conditions) and determined the *J* integral value, which was then converted into a stress intensity factor, K_I, using the relationship $K_I = (J E)^{1/2}$. For a given specimen, a geometric correction factor, $f(a/w)$, can be determined, which for the SENT geometry shown in Fig. 1 is given by:

$$K_I = \sigma_0 \sqrt{\pi a}\, f(a/w) \qquad (1)$$

$$f(a/w) = 2.694(a/w)^3 - 1.949(a/w)^2 + 1.327(a/w) + 1.008)$$

Here K_I is the stress intensity factor for a given geometry, load, and crack size, σ_0 is the remote nominal stress (load divided by gross cross sectional area), a is the crack size, w is the specimen width, and $f(a/w)$ is the geometric correction factor. Using eq (1), loads from the testing machine data, and crack sizes from the videotape images (at initiation of growth and during subsequent growth), the stress intensity factor during each of the SENT tests could be determined.

The surface cracked specimens were more difficult to analyze, because although the crack width could be measured using the videotape images, the crack depth could not. As a result, the examination of surface crack fracture phenomena was limited to determination of the stress intensity factor at the initiation of growth, when we knew both crack width and depth. For these calculations, we used the correction factors for semielliptical surface flaws determined by Newman and Raju [6]. Based on this analysis, the stress intensity for the initial crack size shown is related to the loading through $K_I = \sigma_0 \sqrt{\pi a}(0.6720)$.

Fracture Initiation Toughness

We must emphasize that these composites do not behave like more conventional engineering materials. The composite material can sustain high strains (typically 30%), and experiences clearly visible blunting before growth. As a specimen is stretched, increasing loads cause higher stresses near the crack tip and promote damage in front of the tip by void nucleation and growth. At some critical point, the crack grows into this damaged region. We define the *initiation fracture toughness* as the stress intensity factor for the crack at the point when this crack growth first occurs. This event is clearly distinguishable, and was the basis for determining the initiation fracture toughness. The overall initiation fracture toughness for the SENT specimens was determined using a regression plot. Here the nominal stress (σ_c) is plotted as the ordinate and $1/[\sqrt{\pi a_c}\, f(a_c/w)]$ is plotted as the abscissa (the subscripts denote the values at the critical time of growth initiation). From eq (1), the line will pass through the origin of the graph and have a slope equal to the initiation fracture toughness:

$$K_C = \frac{\sigma_c}{\dfrac{1}{\sqrt{\pi a}\, f(a/w)}} \qquad (2)$$

Figure 2 shows this plot for the SENT specimens and also for the surface cracked specimens. This way of determining the initiation fracture toughness can be used when different crack sizes or specimen geometries are tested and shows which data points (if any) are inconsistent with the other data. Figure 2 shows that the data from the shortest of the crack sizes tested (a_0 = 2.54 mm) disagree with the other results, so the short crack results are not incorporated into the least-squares curve fit of the data. For these very short cracks it is likely that fundamental assumptions inherent in eqs (1) and (2) are violated, since these crack sizes are probably on the scale of the damage zone. We used the regression plot to find the approximate size below which linear fracture mechanics cannot be used (from Fig. 2, this threshold is between 2.54 and 5.08 mm, but depends on the materials and conditions encountered). The behavior of these short cracks has no existing fracture mechanics theories to adequately describe their behavior and requires further study.

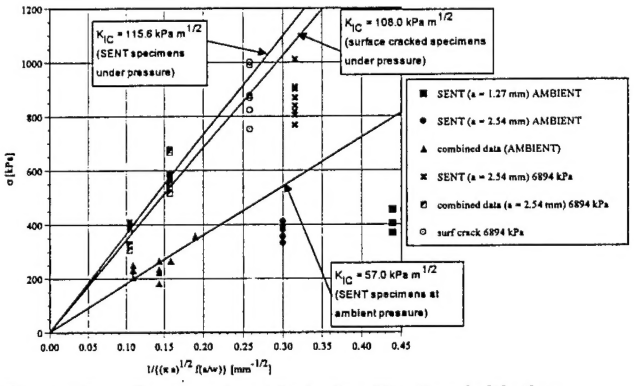

Figure 2 — Regression Plots for Finding Initiation Fracture Toughness

Although we tested three distinct SENT specimen thicknesses (5.08, 12.7, and 38.1 mm), we found no significant thickness effect, and all of the fracture toughnesses were similar. This finding is consistent with previous ambient pressure testing and with damage mechanics research that shows that the development of damage near the crack tip prevents plane strain constraint effects so that no thickness effects are apparent [3].

Figure 2 also shows a regression plot for the surface cracked specimens, as well as previous ambient pressure test results. The surface cracked specimens have similar K_c predictions as the SENT specimens (108.0 and 115.6 kPa √m, respectively), suggesting that the SENT specimens can be used to find the critical values for surface cracks. Furthermore, the effect of pressure is to increase the K_c value of the composite by a factor of about two. One reason for this effect may be that

pressure slows the void nucleation and growth phenomena that in turn inhibits initiation of crack growth.

Crack Growth Calculations

After initiation of growth, the crack begins to accelerate, and we determined the growth rate. We are interested in the growth rate because the crack may grow slowly enough to allow the component to complete its life cycle. Experience with these composites suggests the crack growth rate is governed by a power law of the form:

$$\frac{da}{dt} = CK_I^m \qquad (3)$$

Here *da/dt* is the growth rate, K_I is the stress intensity factor at some point in the growth history, and *C* and *m* are parameters that must be determined [2].

We again see the distinctive behavior of the composite in the crack growth measurements, for, although eq (3) holds in the average sense, it does not accurately model the instantaneous crack speeds. The propagation proceeds by growth into a damaged region, causing crack arrest, followed by blunting and new damage formation near the tip, resulting in more growth. The time variations in *da/dt* complicate the growth analysis, however, the growth rates conform to eq (3) if smoothing techniques are applied to the data before taking time derivatives [1,2,7], so we obtained crack speeds by fitting a polynomial curve to each data set and using the derivative of the polynomial evaluated at each data point as the *da/dt* value. We derived the power law curve that relates crack speeds to stress intensities using the aggregate data obtained from the SENT specimens. The parameters *C* and *m* in eq (3) can be found using a least-squares approach, either by using eq (3) directly or by fitting a line after taking the log of both sides (both methods yield identical results). As Fig. 3 shows, when we did this, we found that $C = 4.833 \times 10^{-6}$ and $m = 2.002$ (assuming units of [mm/s] and [kPa $m^{1/2}$] for *da/dt* and *K*, respectively).

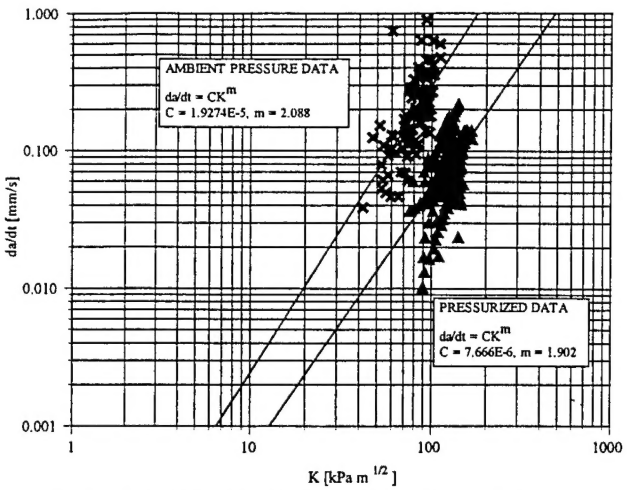

Figure 3 — Determination of Crack Growth Law

Conclusions

We have studied the effects of pressure on the fracture of a rubbery composite. The results show that the single edge notched tension specimens can be used to find the initiation fracture toughness of surface cracks and that pressure raises the stress intensity factor at the initiation of growth. The initiation fracture toughness was determined using a regression method applied to the aggregate data, which has the advantage of showing an approximate minimum crack size for valid application of linear fracture mechanics theories. Testing multiple thicknesses of the specimens reveals that there is no significant thickness effect, a finding supported and suggested by previous work on damage evolution. Finally, a least-squares determination of a power law expression can model the rates of crack growth applied to the aggregate data. The actual growth rates are determined using the time derivatives of polynomial curve fits of the growth versus time data. In the case of crack growth, the effect of pressure was to decrease the growth rates relative to ambient pressure conditions.

References

[1] Liu, C. T., *Effect of Initial Crack Length on Crack Growth*, Abstract Proceedings of Society for Experimental Mechanics Spring Conference on Experimental Mechanics, Bellevue, Washington, pp. 220-221, 1997.

[2] Liu, C. T., *The Effect of Micro Damage on Time-Dependent Crack Growth in a Composite Solid Propellant*, Mechanics of Time-Dependent Materials, Vol. 1, pp. 123-136, 1997.

[3] Liu, C. T. and Miller, T. C., *Effect of Near Tip Damage on the Initiation Fracture Toughness of a Particulate Composite*, ASME Summer Conference on Mechanics and Materials, Symposium on Experiments in Fracture Mechanics, Blacksburg, Virginia, p. 69, 1999.

[4] Miller, T. C., *Analysis of Mixed-Mode Cracks in a Rubbery Particulate Composite*, Composites Part B: Engineering, to be published, 2000.

[5] Cook, R. D., Malkus, D. S. and Plesha, M. E., Concepts and Applications of Finite Element Analysis, 3rd ed., Wiley & Sons, New York, 1989.

[6] Newman, J. C., Jr., *A Review and Assessment of the Stress-Intensity Factors for Surface Cracks*, in Special Technical Publication 687: Part-Through Crack Fatigue Life Prediction, J. B. Chang, ed., American Society for Testing and Materials, pp. 16-42, 1979.

[7] Liu, C. T., *Critical Analysis of Crack Growth Data*, Journal of Propulsion, Vol. 6 no. 5, pp. 519-524, 1990..